Inorg. Chem. **2008**, *47*, 11965−11971

Cu^{2+}-Controlled Hybridization of Peptide Nucleic Acids

János Kovács, Elmar Jentzsch, and Andriy Mokhir*

Anorganisch-Chemisches Institut, Ruprecht-Karls-Universität Heidelberg, Im Neuenheimer Feld 270, 69120 Heidelberg, Germany

Received July 3, 2008

We have prepared cyclic peptide nucleic acids (PNAs). These compounds do not bind complementary nucleic acids. One carboxylic ester group was introduced in the backbone of the cyclic PNAs. This group is cleaved in the presence of Cu^{2+} or coordinatively unsaturated Cu^{2+} complexes. The cleavage products are linear PNAs. In contrast to the cyclic PNAs, they are efficient nucleic acid binders. The rate of formation of the linear PNAs is proportional to the concentration of the cleaving agents. Therefore, one may apply highly sensitive methods of detection of linear PNAs for determination of Cu^{2+} concentration. In particular, we have demonstrated that both fluorescent spectroscopy in combination with molecular beacons and MALDI-TOF mass spectrometry are suitable for the detection of Cu^{2+}. A range of related divalent metal ions and Eu^{3+}, Ln^{3+}, Pr^{3+}, Ce^{3+}, and Zr^{4+} do not interfere with Cu^{2+} detection.

Introduction

The binding of two single-stranded nucleic acids to each other (hybridization) typically correlates with the presence of complementary sequences in the strands. Hybridization is the key step in all existing methods of sequence-specific analysis of nucleic acids. It acts as the trigger of further catalytic reactions that amplify the signal.[1] The sensitivity of detection of hybridization events is high. Therefore, it is of interest to prepare nucleic acids or their analogues whose affinity to nucleic acids is controlled by other important analytes: proteins, drugs, cofactors, and metal ions. This would allow detection of these compounds by monitoring the hybridization and dissociation of nucleic acids. Several approaches based on this principle have been reported. In particular, Nutiu and Li have prepared the duplex, which consists of 5′-fluorophore-DNA, 3′-quencher-DNA, and a DNA template.[2] The template includes an ATP aptamer sequence, which is complementary to the 3′-quencher-DNA, and another sequence, which is complementary to the 5′-fluorophore-DNA. In the duplex, the fluorophore is located in proximity to the quencher and does not fluoresce. In the presence of ATP, the aptamer sequence of the template is folded around ATP, releasing the 3′-quencher-DNA. The resulting increase of fluorescence intensity correlates with ATP concentration.[2] The second example includes the application of nucleic acid based enzymes (DNA/RNAzymes) in metal ion analysis. Catalytically active conformations of these compounds are stabilized by intramolecular hybridizations, which are strengthened and, in some cases, switched on by metal ions. DNA/RNAzymes dependent on Pb^{2+}, Mg^{2+}, Ca^{2+}, Cu^{2+}, Zn^{2+}, and Hg^{2+} have been reported. These ions can be detected by monitoring the catalytic activity of the enzymes.[3] Finally, we have reported Zn^{2+}-, Ni^{2+}-, and Cu^{2+}-dependent, terminally modified peptide nucleic acids (PNAs).[4] An uimportant disadvantage of our compounds is that the metals do not act as true switches of the hybridization except of 5-mer PNAs. These short PNAs have low affinity to complementary nucleic acids and, therefore, cannot be used in combination with usual hybridization probes, for example, molecular beacons.

The ability of oligonucleotides and their analogues to bind nucleic acids can be strongly reduced by chemical modifications of their backbones, bases, or termini. When the modifications are removed, the oligonucleotides regain their nucleic acid affinity. This is used, for example, in the preparation of "caged" nucleic acid binders, whose hybrid-

* Author to whom correspondence should be addressed. E-mail: Andriy.Mokhir@urz.uni-heidelberg.de.

(1) Schweitzer, B.; Kingsmore, S. *Curr. Opin. Biotechnol.* **2001**, *12*, 21–27.

(2) Nutiu, R.; Li, Y. *Chem.—Eur. J.* **2004**, *10* (8), 1868–1876.

(3) (a) Li, J.; Lu, Y. *J. Am. Chem. Soc.* **2000**, *122*, 10466–10467. (b) Lu, Y. *Chem.—Eur. J.* **2002**, *8* (20), 4588–4596. (c) Liu, J.; Lu, Y. *J. Am. Chem. Soc.* **2007**, *129*, 9838–9839.

(4) (a) Boll, I.; Kovbasyuk, L.; Kraemer, R.; Mokhir, A. *Bioorg. Med. Chem. Lett.* **2006**, *16* (10), 2781–2785. (b) Mokhir, A.; Kraemer, R.; Wolf, H. *J. Am. Chem. Soc.* **2004**, *126* (20), 6208–6209.

10.1021/ic8012377 CCC: $40.75
Published on Web 11/17/2008

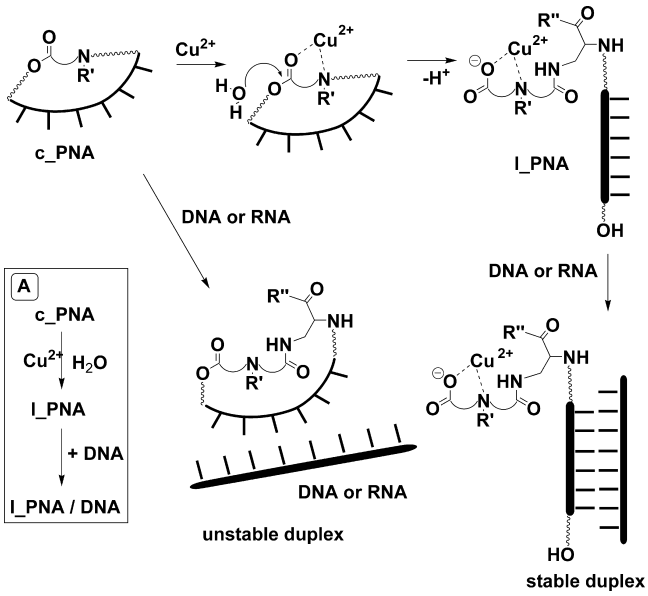

Figure 1. Cu^{2+}-controlled hybridization of peptide nucleic acids with complementary nucleic acids. "R" is a variable group; c_PNA, cyclic PNA; l_PNA, linear PNA; product of c_PNA hydrolysis (inset A).

ization ability is controlled by light.[5] Cyclization of nucleic acid binders may be an alternative general strategy for controlling their hybridization. We have recently demonstrated that the cyclization of PNAs using optimized linkers leads to a complete loss of their ability to hybridize.[6] This ability is restored when one of the chemical bonds in the backbone is cleaved, producing a linear binder (l_PNA). We have used an ester containing a metal-anchoring donor atom as a cleavable group and Cu^{2+} salts as cleaving reagents (Figure 1). The activated linear PNAs were detected by using MALDI-TOF mass spectrometry or fluorescence spectroscopy in combination with molecular beacons. The latter reagents are not fluorescent until they hybridize with single-stranded nucleic acids or their analogues.[7] We have applied the cyclic PNAs in the analysis of Cu^{2+}.[6] These compounds are chemodosimeters, since they accumulate the dose in response to the analyte (Cu^{2+}) and are irreversible.[8] We and others have reported several Cu^{2+} chemodosimeters based on low-molecular-weight dyes.[9] The advantage of the current system is in its versatility. In particular, one can select any molecular beacon for monitoring Cu^{2+}-catalyzed c_PNA hydrolysis. No additional synthesis is required since beacons with a variety of fluorophore-quencher pairs are commercially available. Consequently, tuning the emission wavelength for optimal application-dependent requirements is straightforward. The tuning may be useful for reducing or accounting for the background autofluorescence in the analysis of the metal ions in biological samples, for example, in cell lysates.[10] Cu^{2+} analysis may become important in the sequence-specific detection of nucleic acids. In particular, a proportional amount of Cu^{2+} is released from metallo-DNA probes upon their hybridization to complementary nucleic acids.[11]

Herein, we present further optimization of the cyclic PNAs. In particular, we have determined a binding mode of Cu^{2+} in its complex with **c_PNA4**. **c_PNA4** contains a picolinic acid ester fragment in the linker, which first binds Cu^{2+} and then is hydrolyzed. It is the most Cu^{2+}-sensitive compound in the earlier reported series of cyclic PNAs.[6] On the basis of information on the Cu^{2+} binding mode in the Cu^{2+}–**c_PNA4** complex, we have modified the structure of **c_PNA4** to increase its Cu^{2+} sensitivity further. In particular, several fragments containing one or more donor nitrogen atoms were attached in close proximity to the ester group of the cyclic PNA. Finally, we have applied the cyclic PNA with the best Cu^{2+} sensitivity (**c_PNA8**) in the assay for the metal-ion-specific and -sensitive detection of Cu^{2+}.

Experimental Section

The best commercially available chemicals from Aldrich/Sigma/Fluka (Germany) and Novabiochem (Switzerland) were obtained and used without purification. HPLC-purified DNA was obtained from Metabion (Germany) or IBA (Germany). The reagents for PNA synthesis were obtained from Applied Biosystems (Germany). MALDI-TOF mass spectra were recorded on a Bruker BIFLEX III spectrometer. The solution of 3,5-dimethoxy-4-hydroxycinnamic acid (27 mM in 1% TFA/33.9% CH_3CN/33% MeOH/33% H_2O) was used as a matrix for MALDI-TOF analysis of the PNA conjugates. Samples for mass spectrometry were prepared manually using a dried droplet method with a 1:2 probe/matrix ratio for water and water/CH_3CN solutions (HPLC fractions) and a 1:20 ratio for TFA/*m*-cresol (4:1) solutions. Mass accuracy with external calibration was 0.1% of the peak mass, that is, ±3.0 at *m*/*z* 3000. Preparative and analytical HPLC were performed at 49 °C on a Shimadzu liquid chromatograph equipped with a UV–vis detector and column oven. A Macherey-Nagel Nucleosil C4 250 × 4.6 mm column with gradients of CH_3CN (0.1% TFA, solvent B) in water (0.1% TFA, solvent A) was used, under the following conditions: 49 °C, 0% B for 5 min, in 30 min to 35% B, in 10 min to 90% B, 90% B for 10 min.

Synthesis. The PNA part of conjugates was synthesized on an Expedite 8909 PNA/DNA synthesizer according to the manufacturer's recommendations for 2 μmol scale synthesis. Amino acid residues were attached using commercially available building blocks: Fmoc-Lys(Boc)-OH (lysine residue), Fmoc-DPR(Alloc)-

(5) (a) Monroe, W. T.; Haselton, F. R. Light reversible suppression of DNA bioactivity with cage compounds. In *Dynamic Studies in Biology Phototriggers, Photoswitches and Caged Biomolecules*; Goeldner, M., Givens, R., Eds.; Wiley-VCH: New York, 2005; pp 513–531. (b) Rotaru, A.; Mokhir, A. *Angew. Chem., Int. Ed.* **2007**, *46* (32), 6180–6183; *Angew. Chem.* **2007**, *119* (32), 6293–6296.
(6) Kovács, J.; Roedler, T.; Mokhir, A. *Angew. Chem., Int. Ed.* **2006**, *45* (46), 7815–7817; *Angew. Chem.* **2006**, *118* (46), 7979–7981.
(7) Tyagi, S.; Kramer, F. R. *Nat. Biotechnol.* **1996**, *14* (3), 303–308.
(8) (a) Wolfbeis, O. S. In *Fiber Optic Chemical Sensors and Biosensors*; Wolfbeis, O. S., Ed.; CRC Press: Boca Raton, FL, 1991; Vol I, p 2. (b) Chae, M.-Y.; Czarnik, A. W. *J. Am. Chem. Soc.* **1992**, *114*, 9704–9705.
(9) (a) Qi, X.; Jun, E. J.; Xu, L.; Kim, S.-J.; Hong, J. S. J.; Yoon, Y. J.; Yoon, J. *J. Org. Chem.* **2006**, *71*, 2881. (b) Dujols, V.; Ford, F.; Czarnik, A. W. *J. Am. Chem. Soc.* **1997**, *119*, 7386–7387. (c) Kierat, R. M.; Kraemer, R. *Bioorg. Med. Chem. Lett.* **2005**, *15*, 4824–4827. (d) Kovács, J.; Mokhir, A. *Inorg. Chem.* **2008**, *47* (6), 1880–1882. (e) Mokhir, A.; Kraemer, R. *Chem. Comm.* **2005**, 2244–2245. (f) McCall, K. A.; Fierke, C. A. *Anal. Biochem.* **2000**, *284*, 307–315. (g) Chavez-Crooker, P.; Garrido, N.; Ahearn, G. A. *J. Exp. Biol.* **2001**, *204*, 1433–1444. (i) Breuer, W.; Epsztejn, S.; Millgram, P.; Cabantchik, I. Z. *Am. J. Physiol.* **1995**, *268* (6 Pt 1), C1354–1361.
(10) Billinton, N.; Knight, A. W. *Anal. Biochem.* **2001**, *291*, 175–197.
(11) Graf, N.; Goeritz, M.; Kraemer, R. *Angew. Chem., Int. Ed.* **2006**, *45* (24), 4013–4015; *Angew. Chem.* **2006**, *118* (24), 4117–4119.

OH (2,3-diaminopropionic acid residue), Fmoc-His(Mtt)-OH (histidine residue), Fmoc-Asp(Alloc)-OH (aspartic acid residue), and Fmoc-Glu(Alloc)-OH (glutamic acid residue).

Compound 3a. 2,5-Pyridine dicarboxylic acid (1 g, 6.0 mmol) in DMF (120 μL) was slowly added to $SOCl_2$ (7.2 mL, 99.3 mmol). The mixture was brought to reflux, which led to complete dissolution of the acid. Excess thionyl chloride was removed by evaporation under high vacuum conditions (0.01 mbar), and the rest was dissolved in diethyl ether (30 mL). Allyl alcohol (4.1 mL, 60 mmol) was added to this solution, and the mixture was stirred for 3 h at 22 °C. The precipitate formed was filtered, washed with diethyl ether, and dried. The yield of **3a** was 1.1 g (72%). TLC (eluent CH_2Cl_2/EtOAc 1:1, v/v with 1% NEt_3) $R_f = 0.9$. ESI MS+ found: *m/z* 248.01. Calcd for $C_{13}H_{14}NO_4$: $[M + H]^+$ 248.08. ^{1}H NMR ($CDCl_3$, 200 MHz): δ 4.89 (m, 4H), 5.29−5.48 (m, 4H), 5.93−6.16 (m, 2H), 8.20 (dd, 1H), 8.44 (dd, 1H), 9.32 (dd, 1H). ^{13}C NMR ($CDCl_3$, 50.3 MHz): δ 66.77, 67.49, 119.68, 120.02, 125.52, 129.64, 130.93, 130.95, 140.71, 148.35, 148.96, 162.14, 162.88.

Compound 3b. Compound **3b** was prepared analogously to compound **3a**. 2,4-Pyridine dicarboxylic acid (1 g, 6.0 mmol) was used as the starting material. The yield of **3b** was 1.2 g (83%). TLC (eluent CH_2Cl_2/EtOAc 1:1, v/v with 1% NEt_3) $R_f = 0.9$. ESI MS+ found: *m/z* 247.99. Calcd for $C_{13}H_{14}NO_4$: $[M + H]^+$ 248.08. ^{1}H NMR ($CDCl_3$, 200 MHz): δ 4.96 (m, 4H), 5.34−5.54 (m, 4H), 5.94−6.22 (m, 2H), 8.46 (dd, 1H), 8.84 (dd, 1H), 9.24 (dd, 1H). ^{13}C NMR ($CDCl_3$, 50.3 MHz): δ 67.62, 68.14, 120.43, 120.57, 125.94, 128.21, 130.66, 130.78, 142.92, 144.45, 147.95, 160.77, 162.30.

Compound 4a. Diester **3a** (937 mg, 3.8 mmol) was added to an aqueous $CuCl_2$ solution (0.1 M, 114 μL). The mixture was heated to 50 °C and left for 12 h at this temperature. A light blue precipitate was formed. It was filtered, washed with water, and dried. The solid obtained was dissolved in trifluoroacetic acid (4.5 mL), and H_2S gas was purged through this solution until the blue color disappeared. The precipitate was filtered, and the filtrate was evaporated to dryness. The yield of **4a** was 289 mg (37%). TLC (eluent CH_2Cl_2/MeOH 1:1, v/v) $R_f = 0.7$. ESI MS+ found: *m/z* 208.18. Calcd for $C_{10}H_{10}NO_4$: $[M + H]^+$ 208.96. ^{1}H NMR (TFA-d1, 400 MHz): δ 5.11 (d, 2H), 5.50−5.60 (m, 2H), 6.06−6.17 (m, 1H), 8.94 (d, 1H), 9.52 (d, 1H), 9.71 (d, 1H). ^{13}C NMR (TFA-d1, 100.6 MHz): δ 69.48, 120.95, 128.58, 133.62, 144.25, 149.46. C, H, N analysis (%) found: C, 57.37; H, 4.47; N, 6.61. Calcd for $C_{10}H_{10}NO_4$: C, 57.97; H, 4.38; N, 6.76.

Compound 4b. Compound **4b** was prepared analogously to compound **4a**. Diester **3b** (1 g, 3.5 mmol) was used as the starting material. The yield of **4b** was 375 mg (45%). TLC (eluent CH_2Cl_2/MeOH 1:1, v/v) $R_f = 0.8$. ESI MS+ found: *m/z* 208.03. Calcd for $C_{10}H_{10}NO_4$: $[M + H]^+$ 208.96. ^{1}H NMR (TFA-d1, 400 MHz): δ 5.13 (m, 2H), 5.51−5.61 (m, 2H), 6.09−6.19 (m, 1H), 9.02 (d, 1H), 9.31−9.32 (m, 2H). ^{13}C NMR (TFA-d1, 100.6 MHz): δ 69.66, 120.03, 127.88, 128.59, 131.01, 144.51, 148.71. C, H, N analysis (%) found: C, 57.90; H, 4.55; N, 6.49. Calcd for $C_{10}H_{10}NO_4$: C, 57.97; H, 4.38; N, 6.76.

PNA Cleavage, Deprotection, and Workup. The resin-bound PNA conjugate (0.5−2 μmol) was treated with the TFA/*m*-cresol mixture (4:1 v/v, 120 μL) for 90 min. Then, the resin was filtered off and the filtrate mixed with diethylether (2.5 mL), and the precipitate formed was filtered, washed with diethyl ether (2 × 1 mL), dried (0.01 mbar), and HPLC-purified.

Reductive Amination. A solution of 2-pyridinecarboxaldehyde (9.5 μL, 100 μmol) in CH_2Cl_2 (1 mL) and solid Na_2SO_4 (3 mg) were added to resin containing free amino groups (0.5−2 μmol). The reaction was left shaking at 22 °C for 24 h. The resin was filtered, washed with DMF (4 × 1 mL) and CH_3CN (2 × 1 mL), and dried under a vacuum (0.01 mbar). $Na[B(CN)H_3]$ (6.9 mg, 50 μmol) in methanol (1 mL) was added to the resin, and after 3 h, the resin was filtered, washed with DMF (4 × 1 mL) and CH_3CN (2 × 1 mL), and dried under a vacuum (0.01 mbar).

c_PNA3. HPLC $R_t = 23.3$ min. Yield: 0.43%. MALDI-TOF MS calcd for $C_{121}H_{160}N_{60}O_{30}$ $[M + H]^+$: 2933.3. Found: 2933.5.

c_PNA5. HPLC $R_t = 45.6$ min. Yield: 0.3%. MALDI-TOF MS calcd for $C_{118}H_{152}N_{60}O_{29}$ $[M + H]^+$: 2874.9. Found 2877.3.

c_PNA6. HPLC $R_t = 45.9$ min. Yield: 0.2%. MALDI-TOF MS calcd for $C_{118}H_{152}N_{60}O_{29}$ $[M + H]^+$: 2874.9. Found 2877.3.

c_PNA7. HPLC $R_t = 28.3$ min. Yield: 0.58%. MALDI-TOF MS calcd for $C_{121}H_{159}N_{61}O_{31}$ $[M + H]^+$: 2962.3. Found 2963.3.

c_PNA8. HPLC $R_t = 27.4$ min. Yield: 0.47%. MALDI-TOF MS calcd for $C_{124}H_{160}N_{62}O_{31}$ $[M + H]^+$: 3013.3. Found 3015.2.

c_PNA9. HPLC $R_t = 31.8$ min. Yield: 0.5%. MALDI-TOF MS calcd for $C_{123}H_{156}N_{60}O_{30}$ $[M + H]^+$: 2953.3. Found 2955.5.

Determination of PNA Concentration. HPLC-purified PNAs were lyophilized and dissolved in water (200 μL). A portion of the solution (5 μL) was diluted to 555 μL with water, and UV absorbance at 260 nm was measured. This value was used for calculation of the PNA concentrations. Extinction coefficients of PNAs were calculated as the sum of extinction coefficients of the corresponding nucleobases.

Assays for Monitoring c_PNA Hydrolysis. a. MALDI-TOF Mass Spectrometry. Solutions of cPNA (1 μM) in 10 mM MOPS at pH 7 and 50 mM NaCl containing the corresponding metal ions (0.3, 1, 3, and 10 μM) were prepared at 22 °C. The reaction was started by heating these solutions to 40 °C. Probes (1 μL) were taken at definite times and mixed with a 3,5-dimethoxy-4-hydroxycinnamic acid matrix (2 μL). The resulting mixture was spotted on a MALDI plate and allowed to dry. Prepared in such a way, probes were analyzed by MALDI-TOF mass spectrometry. Each reaction was repeated at least three times.

b. Fluorescence Spectroscopy. Solutions of cPNA (1 μM) in 10 mM MOPS at pH 7 and 50 mM NaCl were prepared at 22 °C. These solutions were treated with $CuSO_4$ (1 μM) at 37 °C for 40 min. Then ethylene-diaminetetracetic acid (3 μM) and DNA Tamra-CCT-TTA-GTT-GTG-AAA-GG-Dabcyl were added, and the intensity of fluorescence at 581 nm was measured (λ_{ex} 560 nm).

Results and Discussion

Synthesis of Cyclic PNAs. Cyclic PNAs have been prepared previously by using a fully backbone-protected strategy.[12] In this method, the cyclic poly-(2-aminoethylglycineamide) precursor is first prepared by sequential coupling of the corresponding monomers in solution. The secondary amino groups in the backbone carry orthogonal protecting groups. There are as many of these groups as there are nucleobases in the target cyclic PNA. A series of selective deprotection−coupling steps allows the simultaneous introduction of the required number of identical nucleobases onto the backbone. This approach has been used for the preparation of 6-mer mixed-sequence cyclic PNAs.

We have chosen an alternative strategy for the preparation of cyclic PNAs, which relies on solid-phase synthesis. The important advantage of our method is that structural modifications can be quickly introduced within the cyclic PNAs that allow optimization of the PNAs' properties within a reasonable time. Moreover, the cyclic PNAs with long

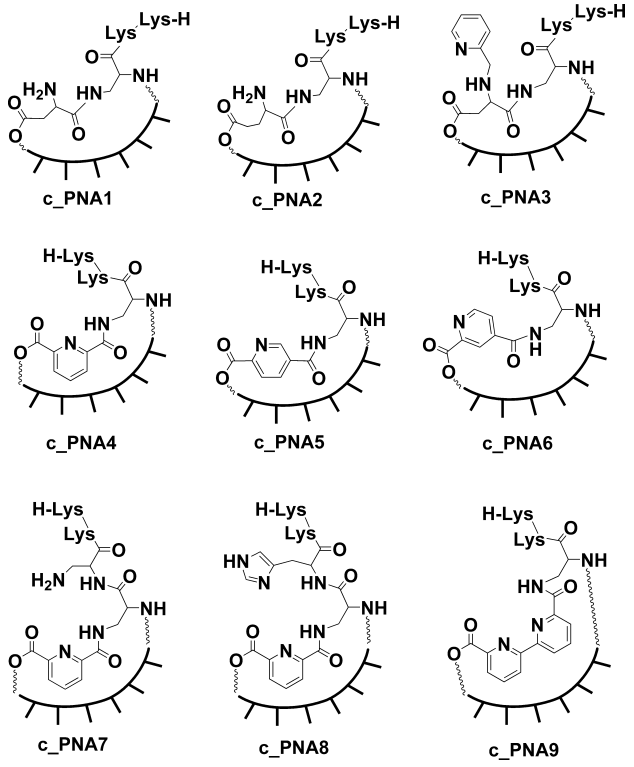

Figure 2. Structures of the linkers introduced within the cyclic PNAs. Gray-colored compounds have been reported previously.[6]

Scheme 1. Synthesis of **c_PNA3**[a]

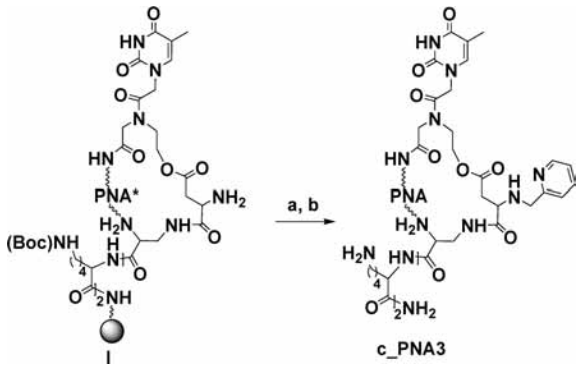

[a] Intermediate **I** was prepared according to ref 6. PNA* is the protected and PNA the deprotected peptide nucleic acid: CAC AAC TA. (a) 2-Pyridinecarboxyaldehyde, $Na[B(CN)H_3]$. (b) TFA, *m*-cresol.

sequences could be routinely prepared. The syntheses of **c_PNA1**, **c_PNA2**, and **c_PNA4** were described in our first communication.[6] Six new cyclic PNAs have been obtained (Figure 2). In particular, **c_PNA3** was prepared from intermediate **I**[6] by reductive amination using 2- pyridinecarboxaldehyde and $Na[B(CN)H_3]$, which was followed by deprotection and cleavage of the PNA from the solid support (Scheme 1). 2-Carboxy-4(5)-allylcarboxypyridines (**4a** and **4b**), which were necessary for the syntheses of **c_PNA5** and **c_PNA6**, were prepared from corresponding unprotected dicarboxylic acids in accordance with Scheme 2. First,

Scheme 2. Synthesis of 2-Carboxy-4-allylcarboxypyridine (**4a**) and 2-Carboxy-5-allylcarboxypyridine (**4b**)[a]

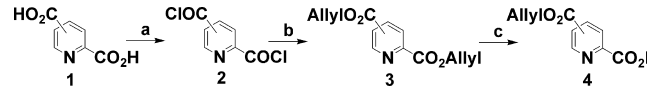

[a] (a) $SOCl_2$, DMF. (b) Allyl-OH, Et_2O. (c) 1: $CuCl_2$, H_2O. 2: H_2S, CF_3CO_2H.

Scheme 3. Synthesis of **c_PNA5, c_PNA6**[a]

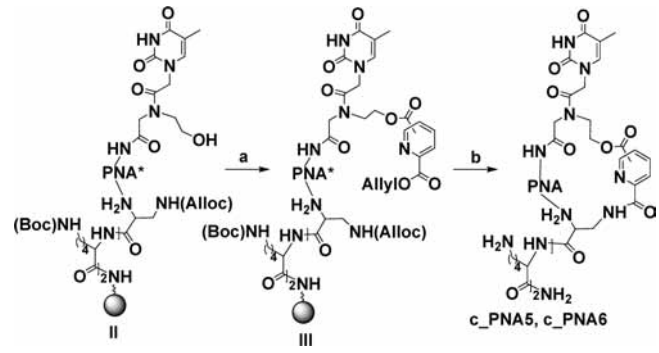

[a] Intermediate **II** was prepared according to ref 6. PNA* is the protected and PNA the deprotected peptide nucleic acid: CAC AAC TA. (a) **4a** (**c_PNA5**) or **4b** (**c_PNA6**), DIC, HOBT, DMAP, DMF. (b) 1: $Pd(PPh_3)_4$, PPh_3, $(Et_2NH_2)(HCO_3)$, CH_2Cl_2. 2: DIC, HOBT, DMAP, DMF. 3: TFA, *m*-cresol (inset A).

Scheme 4. Synthesis of **c_PNA7** and **c_PNA8**[a]

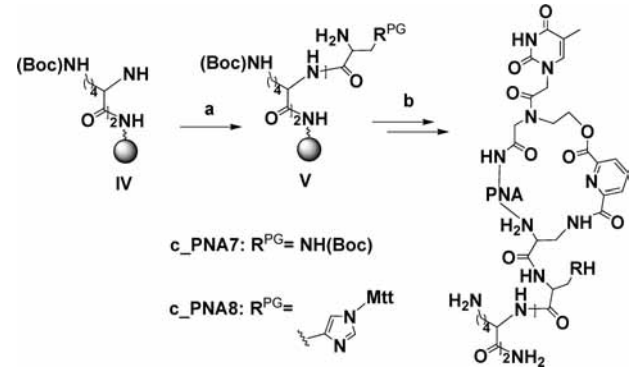

[a] Intermediate **IV** was prepared according to ref 6. (a) Fmoc-DPR(Boc)-OH (**c_PNA7**) or Fmoc-His(Mtt)-OH (**c_PNA8**), HBTU, HOBT, DIEA, DMF. (b) Analogously to the synthesis of **c_PNA4**.[6]

exhaustive esterification was conducted, which was followed by the Cu^{2+}-catalyzed hydrolysis of the ester group neighboring the nitrogen atom of the pyridine fragment. Cu^{2+} was removed from the solution by its precipitation with H_2S. After evaporation of the solvent, analytically pure monosubstituted acids (**4a** or **4b**) were obtained. These acids were coupled to precursor **II**[6] in the presence of a DIC and HOBT activating mixture (Scheme 3). The resulting compound (**III**) was treated with $[Pd(PPh_3)_4]$ to simultaneously remove alloc and allyl protecting groups, then with DIC to induce cyclization, and finally, with TFA and *m*-cresol to deprotect and cleave **c_PNA5** and **c_PNA6** from the solid support. **c_PNA7** and **c_PNA8** were obtained analogously to **c_PNA4**[6] except that an additional amino acid residue (2,3-diaminopropionic acid, **c_PNA7**, and histidine, **c_PNA8**) was attached to intermediate **IV** (Scheme 4). **c_PNA9** was also obtained analogously to **c_PNA4**[6] except that 2,2′-bipyridine-

(12) (a) Depecker, G.; Patino, N.; Di Giorgio, C.; Terreux, R.; Cabrol-Bass, D.; Bailly, C.; Aubertin, A.-M.; Condom, R. *Org. Biomol. Chem.* **2004**, *2*, 74–79. (b) Upert, G.; Mehiri, M.; Goddard, M.-L.; Di Giorgio, A.; Benhida, R.; Condom, R.; Patino, N. *Tetrahedron Lett.* **2005**, *46*, 4081–4085.

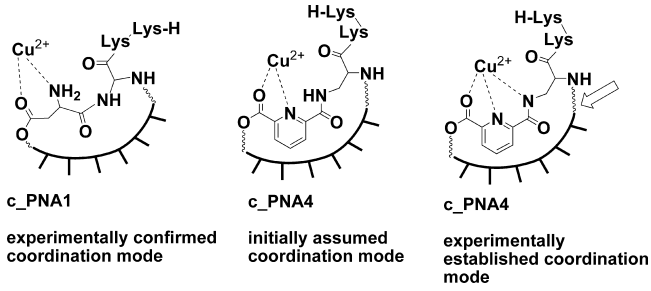

Figure 3. Experimentally observed (**c_PNA1**), initially assumed (**c_PNA4**), and finally established (**c_PNA4**) modes of Cu^{2+} coordination to the cyclic PNAs. Open arrow indicates the site in the PNA for introducing additional donor atoms to increase its affinity toward Cu^{2+}.

6,6′-dicarboxylic acid was used in place of pyridine-2,6-dicarboxylic acid.

Cu^{2+} Binding Site in c_PNA4. Cu−O(ester) coordination strongly polarizes the ester groups and makes them susceptible to hydrolysis, even at pH 7. We have recently investigated a series of cyclic PNAs containing a range of the ester groups in the linker. We have found that these groups can be cleaved by $[Cu^{2+}] < 10$ μM, provided that (a) the metal ion coordination site within the PNA includes O(ester) and an additional donor nitrogen atom and (b) the formation of stable five- or six-atom chelate metallocycles is possible.[6] Within this series, the PNA with a picolinic ester fragment (**c_PNA4**) was the most Cu^{2+}-sensitive compound (Figure 2). Since it was less synthetically challenging, we have investigated first a mode of Cu^{2+} binding to **c_PNA1**.[6] Then, we have assumed that, analogously to **c_PNA1**, **c_PNA4** coordinates Cu^{2+} in a bidentate fashion via oxygen and nitrogen donor atoms (Figure 3). However, the rate of catalytic hydrolysis of **c_PNA4** (1 μM) in the presence of 300 nM Cu^{2+} turned out to be ∼5 times faster than its spontaneous hydrolysis rate. In contrast, **c_PNA1** is not hydrolyzed at all under these conditions. This indicates that Cu^{2+} forms a substantially more stable complex with **c_PNA4** than with **c_PNA1**, which could not be explained on the basis of our initial assumption. We have further hypothesized that, together with Cu^{2+}−(N,O) binding, **c_PNA4** may coordinate Cu^{2+} via at least one additional donor atom: in the O, N, X-coordination mode. The most probable X is a nitrogen atom of the amide group (Figure 3). It has been reported that, when included in a polydentate ligand, the amide group may tightly bind Cu^{2+}.[13] This process is accompanied by deprotonation of the amide. To test whether the amide of **c_PNA4** is coordinated to the metal ion, we have prepared two **c_PNA4** analogues: **c_PNA5** and **c_PNA6**, which contain 2,5- (**c_PNA5**) and 2,4-pyridine (**c_PNA6**) residues in place of the 2,6-substituted pyridine. In these PNAs, coordination of the amide group to Cu^{2+} is not possible. Both **c_PNA5** and **c_PNA6** are substantially less sensitive to Cu^{2+} than **c_PNA4**. In particular, rates of **c_PNA5** and **c_PNA6** hydrolysis with a 30-fold excess of Cu^{2+} are equal to the rate of **c_PNA4** hydrolysis in the presence of only a 3-fold excess of Cu^{2+} (Figure 4). These data confirm that Cu^{2+} in its complex with **c_PNA4** is coordinated to O(ester), N(pyridine), and N(amide) atoms (Figure 3).

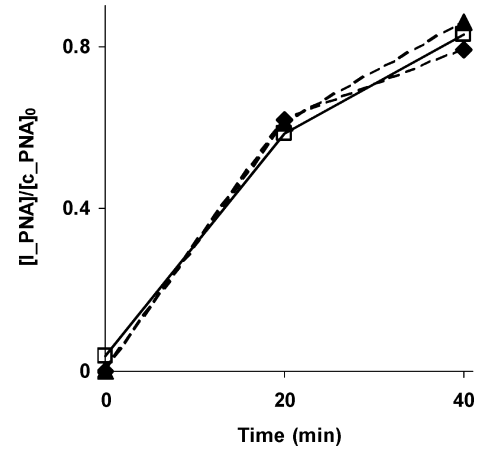

Figure 4. Cleavage of cyclic PNAs containing different picolinic acid ester fragments within the backbone. Conditions: [PNA] = 1 μM, [MOPS] = 10 mM pH 7, [NaCl] = 50 mM, T = 37 °C; open squares - **c_PNA4**, $CuSO_4$ (3 μM); filled diamonds - **c_PNA5**, $CuSO_4$ (30 μM); filled triangles - **c_PNA6**, $CuSO_4$ (30 μM); $[c\_PNA]_0$, concentration of the PNAs at the beginning of the reaction; [l_PNA], concentration of the linear PNAs during the reaction.

Optimization of Sensitivity of Cyclic PNAs toward Cu^{2+}. MALDI-TOF mass spectrometry is a quick (<1 min per probe) and highly sensitive (∼ 100 fmol PNA per spot) method of PNA analysis. It has been used previously for the determination of concentrations of oligodeoxyribonucleotides[14] and peptide nucleic acids[15] in complex mixtures. We have found that the ratio of intensities of c_PNA and l_PNA peaks in MALDI-TOF mass spectra are equal to [c_PNA]/[l_PNA] molar ratios. In particular, this was confirmed by comparison of the MALDI-TOF mass spectra of partially hydrolyzed cPNA mixtures with their HPLC profiles. Such correlation is not surprising since the mass difference between l_PNA's and c_PNA's is only 18 Da and their structures are similar to each other. We have used MALDI-TOF mass spectrometry for the determination of concentrations of c_PNA's and l_PNA's in their mixtures. The typical mass spectra obtained before and after the addition of Cu^{2+} to a cyclic PNA are shown in Figure 5.

In accordance with our data analysis, Cu^{2+} is coordinated to **c_PNA4** via O(ester), N(pyridine), and N(amide) atoms, as shown in Figure 3. On the basis of this information, we could suggest that introducing additional donor atoms at the "C terminus" of the PNA should lead to increasing affinity of the PNA toward Cu^{2+} (the site of the modification is indicated with an arrow in Figure 3). We have prepared two **c_PNA4** analogues with modifications at this site. In particular, **c_ PNA7** contained a 2,3-diaminopropionic acid

(13) (a) Mokhir, A.; Vilaplana, R.; Gonzalez-Vilchez, F.; Fritsky, I. O.; Domasevitch, K. V.; Dudarenko, N. M. *Polyhedron* **1998**, *17* (16), 2693–2697. (b) Sliva, T. Y.; Duda, A. M.; Glowiak, T.; Fritsky, I. O.; Amirkhanov, V. M.; Mokhir, A. A.; Kozlowski, H. *J. Chem. Soc., Dalton Trans.* **1997**, *2*, 273–276.

(14) (a) Mokhir, A.; Connors, W. H.; Richert, C. *Nucleic Acids Res.* **2001**, *29* (17), 3674–3684. (b) Mokhir, A.; Tetzlaff, C. N.; Herzberger, S.; Mosbacher, A.; Richert, C. *J. Comb. Chem.* **2001**, *3* (4), 374–386. (c) Kryatova, O. P.; Connors, W. H.; Bleczinski, C. F.; Mokhir, A.; Richert, C. *Org. Lett.* **2001**, *3* (7), 987–990. (d) Mokhir, A.; Richert, C. *Nucleic Acids Res.* **2000**, *28* (21), 4254–4265.

(15) Boll, I.; Kraemer, R.; Brunner, J.; Mokhir, A. *J. Am. Chem. Soc.* **2005**, *127* (21), 7849–7856.

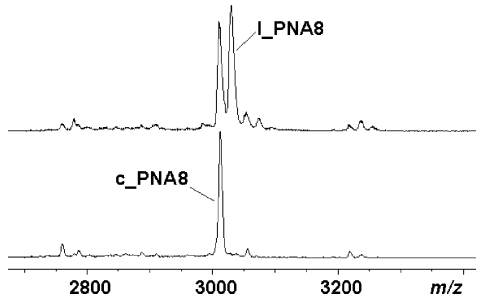

Figure 5. Cleavage of **cPNA8** (1 μM) in the presence of $CuSO_4$ (1 equiv) in aqueous, buffered solution at pH 7 (MOPS 10 mM, NaCl 50 mM) at T = 37 °C. The reaction was monitored by MALDI-TOF mass spectrometry: the lower spectrum was acquired before Cu^{2+} addition; the upper one was acquired 40 min after Cu^{2+} addition.

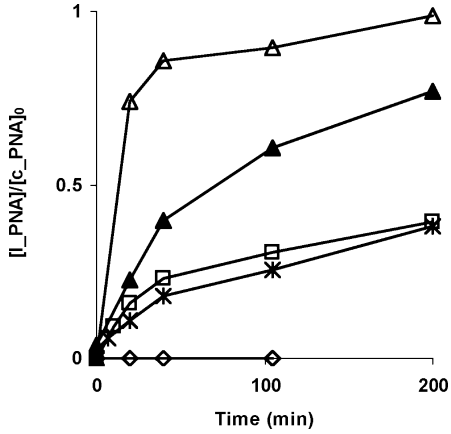

Figure 6. Kinetics of hydrolysis of representative cyclic PNAs (1 μM) under similar conditions: MOPS 10 mM pH 7, NaCl 50 mM, $CuSO_4$ 1 equiv, T = 37 °C; open triangles, **c_PNA8**; filled triangles, **c_PNA4**; open squares, **c_PNA9**; star, **c_PNA7**; open diamonds, **c_PNA8** without Cu^{2+}; hydrolysis of **c_PNAs 4**, **7**, and **9** in the absence of Cu^{2+} overlaps with that of **c_PNA8**. $[c\_PNA]_0$, concentration of the PNAs at the beginning of the reaction; [l_PNA], concentration of the linear PNAs during the reaction.

residue, **c_PNA9**—a histidine residue (Figure 2). Moreover, we have substituted the pyridine for a 2,2′-bipyridine residue to obtain **c_PNA9**. **c_PNAs7** and **c_PNA8** contain potential 5-dentate ligands and **c_PNA9** a potential 4-dentate ligand (Figure 2), whereas the coordination site in **c_PNA4** is only tridentate. Surprisingly, the ester groups of **c_PNA7** and **c_PNA9** exhibit lower Cu^{2+} sensitivity than that of **c_PNA4** (Figure 6). One may speculate that, in these PNAs, there is an alternative high-affinity Cu^{2+} binding site, which is located far away from the ester group. As a consequence, the coordination site with ester−Cu^{2+} interaction is less populated. In contrast to **c_PNAs7** and **c_PNA9**, **c_PNA8** is more sensitive to Cu^{2+} than **c_PNA4**. This indicates that the metal ion in the Cu^{2+}−**c_PNA8** complex, additionally to O(ester), N(pyridine), and N(amide) atoms (as in Cu^{2+}−**c_PNA4**, Figure 3), is coordinated to one or more other donor atoms. We may suggest that the Cu^{2+} coordination sphere includes N(histidine), O(ester), N(pyridine), and two N(amide) atoms, as shown in Figure 7. However, this remains to be confirmed in further structural studies.

Further, we have attempted to improve the sensitivity of **c_PNA1** toward the metal ion. This PNA contains an amino group, which can be easily modified by reductive amination. By using this reaction, we have obtained **c_PNA3**, which

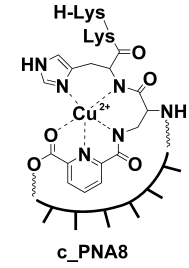

Figure 7. Proposed coordination mode of Cu^{2+} in the Cu^{2+}−**c_PNA8** complex.

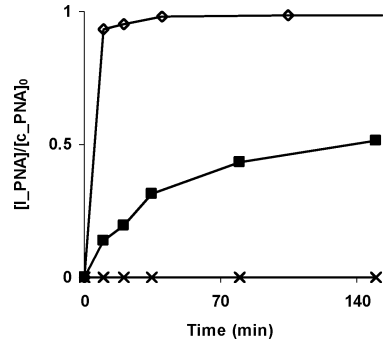

Figure 8. Kinetics of **c_PNA8** (1 μM) hydrolysis in MOPS 10 mM pH 7, NaCl 50 mM buffer at T = 37 °C in the presence of $CuSO_4$ (3 eq) - open diamonds; $CuSO_4$ (3 equiv) and 2,2′-bipyridine (3 equiv) - filled squares; $CuSO_4$ (3 equiv) and 2,2′-bipyridine (6 equiv) - crosses. $[c\_PNA]_0$, concentration of the PNAs at the beginning of the reaction; [l_PNA], concentration of the linear PNAs during the reaction.

contains a 2-picolyl fragment. This PNA is potentially able to bind Cu^{2+} via an oxygen atom (C═O in the ester) and two nitrogen atoms (β-NH and pyridine; Figure 2). As expected, **c_PNA3** turned out to be more susceptible to hydrolysis in the presence of Cu^{2+} than **c_PNA1**. In particular, this compound is hydrolyzed fully only in 20 min in a solution containing 10 equiv of Cu^{2+}. Under these conditions, **c_PNA1** requires 60 min for the same conversion. Unfortunately, the rate of spontaneous hydrolysis of **c_PNA3** is also high. It is only ∼4 times slower than catalytic hydrolysis. In contrast, **c_PNA1** is ∼120 times more stable in the absence of Cu^{2+}. The instability of **c_PNA3** may be caused by intramolecular interaction of the ester group with the nucleophilic nitrogen atom of the pyridine residue.

Cu^{2+} Specificity of the Cyclic PNAs. We have tested the Cu^{2+} specificity of the most sensitive cyclic PNA: **c_PNA8**. This compound is rather specific since it is not responsive to 10-fold excesses of Zn^{2+}, Ni^{2+}, Fe^{2+}, Co^{2+}, Mn^{2+}, Zr^{4+}, Ce^{3+}, Ln^{3+}, Eu^{3+}, and Pr^{3+}, while 1 equiv of Cu^{2+} induces the hydrolysis of >70% of this PNA within 20 min.

Hydrolysis of c_PNA8 Catalyzed by Mono- and Bis-Cu^{2+}-2,2′-bipyridyl Complexes. The hydrolysis of **c_PNA8** (1 μM) in the presence of 3 equiv of Cu^{2+} is fully inhibited by 6 equiv of 2,2′-bipyridyl (bipy; Figure 8). This ligand binds Cu^{2+}, forming the $[Cubipy_2]^{2+}$ complex, where all equatorial positions at the metal ion are occupied (log $\beta_2([Cubipy_2]^{2+}) = 14.7$).[13] $[Cubipy_2]^{2+}$ can bind additionally one or two monodentate ligands in the axial positions. These interactions are weak, and apparently they are not important in the dilute solutions used in our experiments. In the presence of 1 equiv of bipy with respect to Cu^{2+}, the major

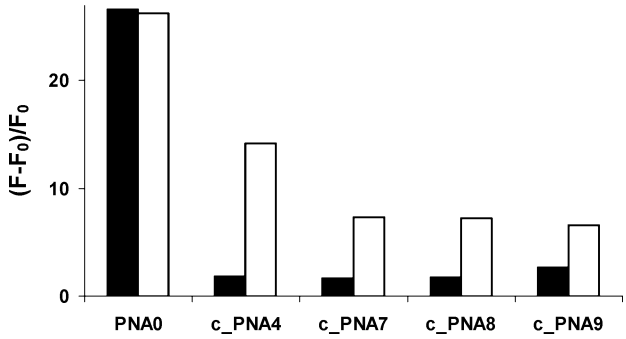

Figure 9. Fluorescence of Tamra-CCT TTA GTT GTG AAA GG-Dabcyl (**MB**) in the presence of selected PNAs: linear **PNA0** (TCA CAA CTA-Lys) and cyclic PNAs **4**, **7**, **8**, **9**; (δ_{ex}= 560 nm, δ_{em}= 581 nm; F_0 is fluorescence of **MB** (100 nM) in MOPS 10 mM pH 7, NaCl 50 mM buffer; F is fluorescence of **MB** after addition of 1 eq PNA; filled bars: no $CuSO_4$ added; open bars: the mixtures were treated first with $CuSO_4$ (10 eq) for 30 min at 37 °C and then with ethylenediaminetetracetic acid (10 eq).

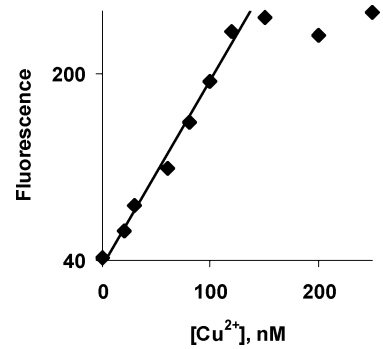

Figure 10. Fluorescence of Tamra-CCT TTA GTT GTG AAA GG-Dabcyl (100 nM), **c_PNA8** (100 nM), MOPS 10 mM pH 7, NaCl 3 mM mixture in the presence of different concentrations of Cu^{2+}. The mixtures were treated first with $CuSO_4$ for 20 min at 37 °C; then, ethylenediamine-N,N,N′,N′-tetracetic acid (500 nM) was added and fluorescence (δ_{ex}= 560 nm, δ_{em}= 581 nm) measured. Solid lines represent linear parts of dependence of fluorescence from Cu^{2+} concentration.

complex in solution is $[Cubipy]^{2+}$ (log $K_1([Cubipy]^{2+})$ = 9.0),[13] which has two "free" (occupied by weakly bound water molecules or anions) equatorial positions. This complex catalyzes the hydrolysis of **c_PNA8**, though not as efficiently as Cu^{2+} does alone (Figure 8). In particular, the initial rate of **c_PNA8** hydrolysis by the complex is reduced by a factor of 10 with respect to that by free Cu^{2+}. Experiments with 2,2′-bipyridyl suggest that not only free Cu^{2+} but also coordinatively unsaturated Cu^{2+} complexes can be analyzed by using the cyclic PNAs. This may be important for practical applications, since Cu^{2+} is often found in the bound form in biological fluids and in environmental samples.

Application of c_PNA8 as a Cu^{2+} Chemodosimeter. Cyclic **c_PNA8** was found to have the highest affinity toward Cu^{2+} among the studied PNAs (Figure 6).[6] Moreover, this compound does not bind complementary nucleic acids in aqueous solution, while Cu^{2+} triggers its transformation to the efficient binder (Figure 9). This optimal PNA was selected for the development of the protocol for Cu^{2+} analysis. The fluorescence of the molecular beacon (Tamra-CCT TTA GTT GTG AAA GG-Dabcyl, 1 μM) and **c_PNA8** (1 μM) mixture, which was treated with different Cu^{2+} concentrations, is shown in Figure 10. The plot is linear at $0 < [Cu^{2+}] \leq 120$ nM (solid straight line). The lowest Cu^{2+} concentration detectable by this method was 30 nM, which corresponds to 1.5 pmol of Cu^{2+} (the total volume of solutions was 50 μL). This is comparable to the best known Cu^{2+} chemodosimeters reported by Yoon et al.,[9a] Czarnik et al.,[9b] Krämer and Kierat,[9c] and Kovács and Mokhir[9d,e] and commercially available Cu^{2+} sensors: Fura-2,[9f] Phen Green,[9g] and Calcein.[9i] When the hydrolysis of **c_PNA8** is monitored by MALDI-TOF mass spectrometry, a lower detection limit (100 fmol) can be achieved. The reason for this is that a smaller solution volume is needed (~1 μL) for the measurement of the MALDI-TOF mass spectrum.

Conclcusions

We have determined the coordination mode of Cu^{2+} in its complex with cyclic peptide nucleic acid containing a picolinic acid ester fragment in the linker, **c_PNA4**. On the basis of this information, we have further modified the **c_PNA4** structure to improve its sensitivity toward Cu^{2+} at pH 7. The optimal PNA, **c_PNA8**, coordinates Cu^{2+} via four nitrogen atoms and one oxygen atom. It is able to bind the metal ion efficiently even at nanomolar concentrations. We have applied **c_PNA8** as a chemodosimeter for Cu^{2+} detection. When fluorescence spectroscopy was used for monitoring the Cu^{2+} concentration, the detection limit was 1.5 pmol of the metal ion, while MALDI-TOF mass spectrometric monitoring improved the detection limit: 100 fmol. A range of related divalent metal ions and Eu^{3+}, Ln^{3+}, Pr^{3+}, Ce^{3+}, and Zr^{4+} do not interfere with Cu^{2+} detection.

Other applications of the related cyclic PNAs are currently being investigated. In particular, we are working on the PNAs whose hybridization ability is controlled by natural hydrolytic enzymes and by visible light.

Acknowledgment. We thank Ruprecht-Karls-Universität Heidelberg, Deutsche Forschungsgemeinschaft (Emmy Noether research group of AM), Alexander von Humboldt Stiftung (Postdoctoral fellowship for J.K.), and Konrad-Adenauer-Stiftung (Ph.D. fellowship for E.J.) for financial support.

IC8012377